Proceedings of the ASME 2010 3rd Joint US-European Fluids Engineering Summer Meeting and 8th International Conference on Nanochannels, Microchannels, and Minichannels
FEDSM-ICNMM2010
August 1-5, 2010, Montreal, Canada

FEDSM-ICNMM2010-31187

NON-NEWTONIAN EFFECTS ON BLOOD FLOW DYNAMICS IN STENTED CORONARY ARTERY BIFURCATIONS

Marjan Molavi Zarandi*
Department of Mechanical Engineering
McGill University
Montreal, Quebec H3A 2K6, Canada
Email: marjan.molavizarandi@mail.mcgill.ca

Rosaire Mongrain
Department of Mechanical Engineering and
McGill University
Montreal, Quebec H3A 2K6, Canada
Email: rosaire.mongrain@mcgill.ca

Olivier F. Bertrand
Faculty of Medicine
Laval University
Quebec City, G1V 4G5, Canada
Email: olivier.bertrand@criucpq.ulaval.ca

Ali Bonakdar
Department of Mechanical Engineering
McGill University
Montreal, Quebec H3A 2K6, Canada
Email: bonakdar@cim.mcgill.ca

ABSTRACT

From clinical practice, it is known that coronary artery bifurcations are regions where the flow is strongly perturbed, and is prone to the development of atherosclerotic lesions.

Bifurcation lesions have always represented a major challenge for placement of stents for treatment of stenosis. Conventional bare metal stents are mostly used in clinical practice of bifurcation lesion treatments since there is no specific commercially available stent dedicated for treating bifurcations.

Stent design is strongly influenced by the specific hemodynamic conditions in a given vessel. Therefore, in principal, what was previously assessed for standard stent design, should be re-assessed for stenting bifurcations. In this paper a blood flow model for stented coronary artery bifurcation is presented. The non-Newtonian approach incorporating blood rheology under low shear rates is presented by employing Carreau model. Computational fluid dynamics modeling is used to adapt the model and characterize the non-Newtonian flow patterns and identify the hemodynamic factors that may influence the stent design. The results shows that the flow conditions and particularly shear stress distribution in the vicinity of stent struts and near arterial wall are significantly different compared to the usually assumed Newtonian flow conditions.

NOMENCLATURE

ρ	density of the fluid
u	velocity vector
v	velocity vectors
p	pressure
τ	stress tensor
μ_∞	viscosity at infinite shear rate
μ_0	viscosities at zero shear rates
η	apparent blood viscosity
λ	time constant
n	power law index
$\dot{\gamma}$	shear rate
V_{max}	maximum velocity
V	velocity

INTRODUCTION

Cardiovascular diseases are defined as pathologies and injuries of the cardiovascular system [1]. Heart, its vessels and

* Corresponding author

the system of blood vessels throughout the body and within the brain are part of the cardiovascular system.

Atherosclerosis is the primary cause of vascular diseases. The current aetiology is the accumulation of lipids and fibrous elements in the arteries. Atherosclerosis reduces arterial lumen size through plaque formation and growth. Clinical studies have also shown that atherosclerotic plaque tends to localize in the vicinity of bifurcations and junctions [2, 3]. Local factors, such as hemodynamic forces and Wall Shear Stress (WSS), play a major role in the localization and development of atherosclerosis [4- 7].

The first evidence implicating WSS in the localization of atherosclerosis was described over 40 years ago by Caro *et al.* [3]. Computational fluid dynamic simulations using autopsy-based models of coronary arteries [5], carotid bifurcations [8] and distal abdominal aortas [9] showed that areas with low WSS correlated with the localization of atherosclerosis.

Open heart surgery was the main method for the treatment of cardiovascular diseases until the early 1960s. Charles Dotter in the 1960s proposed a different approach to treat the disease by developing endovascular therapies. In the early 1980s, Dr. Julio Palmaz began experimenting with thin-walled slotted tubes, stents, which could be expanded by an angioplasty balloon. With this revolutionary contribution, the first Palmaz stent was implanted in human in 1987. Since then, numerous types of stents have been developed and different kinds of materials, designs and techniques have been explored.

Stent implantation changes the arterial blood flow patterns and subsequently changes the magnitude and distribution of shear stress. Peacock *et al.* demonstrated measurable flow disturbances due to stent implantation using an in vitro pulse duplication system [10]. Both in vitro and in vivo studies have revealed that stent structure influences global and local flow patterns [11, 12]. Studies of stent-induced changes in artery wall flow patterns, focused on the near-wall flow patterns, revealed very low magnitude of shear rate between the stent struts [13].

Investigation of blood flow hemodynamics and shear forces are of great importance in understanding the regions of disease formation, development and predicting the performance of cardiovascular technologies such as stents. However the study of blood flow hemodynamics requires an in depth understanding of the physics and assumptions toward a realistic physiological modeling.

In principle, the arterial blood flow in the human body corresponds to a multiphase non-Newtonian pulsatile flow regime. However blood behaves like a Newtonian fluid when the shear rate is over a certain threshold. There is a range in the literature on this limiting shear rate that varies between 50 s^{-1} and 300 s^{-1} [14]. In certain regimes within the stent strut, the shear rate is well below 200 s^{-1} possibility reaching non-Newtonian regime [15].

Comparing Newtonian and non-Newtonian blood viscosity models shows that there is significant increase in WSS between two struts for non-Newtonian property of blood [13]. Therefore, in his work Benard *et al.* [13] suggest that blood should be treated as a non-Newtonian fluid to accurately characterize the hemodynamic of a stented arterial segment.

To the best of our knowledge, very few studies have investigated the blood flow hemodynamic into a stented bifurcation. A study of a stented aorto-iliac bifurcation model with pulsatile flow is presented by Fabregues *et al.* [12]. In their study, the non-Newtonian nature of blood is not taken into account. The experimental and numerical characterization of the hemodynamic changes induced by the presence of two stents in a 90 ° bifurcated coronary was investigated by Delpano *et al.* [16]. They studied flow induced WSS for coronary artery bifurcation with unsteady, incompressible and Newtonian flow conditions.

The flow conditions and particularly shear stress distribution in the vicinity of stent struts and near wall in stented coronary artery are expected to be non-Newtonian and consequently different compared to the usually assumed Newtonian flow conditions. This work addresses these issues using an approach incorporating the physiological conditions. An anatomical structure is replicated and two-dimensional Computational Fluid Dynamic (CFD) analysis is carried out for non-Newtonian pulsatile flow to analyze the hemodynamic changes induced by endovascular stents in the coronary artery bifurcation.

MATERIAL AND METHODS

A comprehensive hemodynamic analysis was carried out to obtain the velocity field and associated WSS distribution in a coronary artery bifurcation. The simulation was conducted using COMSOL which is dedicated for various physics and engineering applications amongst CFD analysis. The computational domain was also meshed in this software. The combination of both momentum and continuity equations for transient, Newtonian and non-Newtonian models of the blood flow were analyzed using the same software.

A geometrical model of 45° coronary bifurcation was considered to simulate the left anterior descending coronary artery bifurcation. The parent vessel diameter was 3 *mm* and daughter vessels diameters were 2.5 *mm* and 1.7 *mm* respectively [17]. A generic helical stent geometry composed of a square wire was used. A 2D representation of helical stent was considered by looking at a plane section through the longitudinal axis of the stent. This situation would correspond to a stent made up of a series of successive rings. Two stents were inserted; one in the main vessel and the other one in the daughter vessel. The dimensions for stent struts were 10 struts, 0.1 *mm*, and located 0.7 *mm* center to center apart [18].

For the study of blood flow in the arteries, we assumed that blood can be represented by an incompressible fluid which is governed by the momentum equation:

$$\rho\left(\frac{\partial u}{\partial t} + u.\nabla u\right) = -\nabla p + \nabla.\tau \qquad (1)$$

and the continuity equation:

$$\frac{\partial \rho}{\partial t} + \nabla.\rho u = 0 \qquad (2)$$

where, ρ denotes the density of the fluid ($kg\ m^{-3}$), u the velocity vector ($m\ s^{-1}$), p the pressure (Pa) and τ the stress tensor which is dependent on the viscosity and shear rate. In the most general situation, the arterial blood flow in the human body is a multiphase non-Newtonian pulsatile flow.

To model the non-Newtonian properties of blood, a constitutive equation is necessary to define the relationship between apparent viscosity and shear rate. There are three distinct regions for apparent blood viscosity; a lower Newtonian region (low shear rate constant viscosity, μ_o), an upper Newtonian region (high shear rate constant viscosity, μ_∞), and a middle region where the apparent viscosity is decreasing with increasing shear rate [19]. Various non-Newtonian blood models have been used to show the shear thinning behaviour of blood while meeting the regions of the low and high apparent viscosity. It is generally accepted that blood behaves as a Newtonian fluid for shear rate above 100 s^{-1} [20]. From the various non-Newtonian blood models, the Carreau model approaches the constant Newtonian value at high shear rate and provides the adequate information to model blood behaviour [21].

In the Carreau model, the viscosity is expressed by the equation:

$$\eta = \mu_\infty + (\mu_0 - \mu_\infty)[1 + (\lambda \dot{\gamma})^2]^{\frac{(n-1)}{2}} \qquad (3)$$

where η is the effective apparent blood viscosity, μ_∞ and μ_0 are the blood viscosities at infinite and zero shear rates (*Pa. s*) respectively, $\dot{\gamma}$ is the shear rate (s^{-1}); λ is a time constant and n is a dimensionless parameter determined with experimental fitting [21]. In the Carreau model, the viscosity is dependent on the shear rate ($\dot{\gamma}$) , which for two dimensions is defined according to equation:

$$\dot{\gamma} = [2\{(\frac{\partial u}{\partial x})^2 + (\frac{\partial v}{\partial y})^2\} + (\frac{\partial u}{\partial y} + \frac{\partial v}{\partial x})^2]^{\frac{1}{2}} \qquad (4)$$

where u, v are the velocity vectors, respectively.

To solve the governing equations, a set of boundary conditions is required. In this analysis, the maximum velocity (V_{max}) varies between 24 *cm/s* and 46 *cm/s* for a coronary artery of 3 *mm* in diameter [22]. The flow was considered laminar and fully developed throughout the study section; hence the velocity distribution in the inlet was set to be parabolic as expressed in (5):

$$V = V_{\max}[1 - (\frac{R}{R_a})^2] \qquad (5)$$

where R is the radial position and R_a the inner radius of the artery [23].

Velocity variation was obtained from blood flow rate during the cardiac cycle. Figure 1 shows the variation of the blood flow rate in the left coronary artery during the cardiac cycle [23].

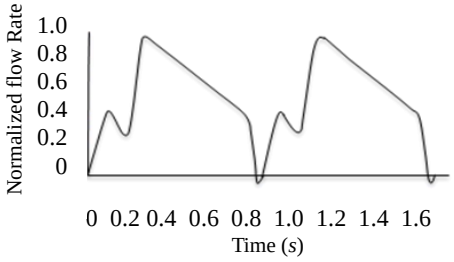

Figure 1. Normalized flow rate waveform for the left main coronary artery.

Pulsatile flow was considered, where the inflow velocity was based on a time-dependent flow rate obtained from Figure 1. The waveform has a period T =0.8 *s* (67 beats per minute), where 0 <*t (sec)* <0.2 is systolic and 0.4 <*t (sec)* <0.9 is diastolic. At the walls, the velocity obeyed the no-slip condition. At the outlet of the daughter vessels, a stress-free condition was assumed as the boundary conditions.

The non-Newtonian blood model, Carreau, was considered in this analysis. The non-Newtonian blood properties in this model are blood viscosity at infinite shear rate μ_∞ =*0.035 mPa.s*, blood viscosities at zero shear rates μ_0=0.56 *mPa.s*, λ=3.313 *s* and n=0.3568 [21]. Blood density is used to ρ =1060 Kg/m^3 [24].

RESULTS

Numerical analysis of pulsatile blood flow in healthy and stented coronary artery bifurcation was carried out for both Newtonian and non-Newtonian flow models. A two-dimensional CFD model of the stented coronary artery bifurcation was developed and the corresponding velocity field and shear stress distributions were investigated. Velocity profiles at five different time steps in a cardiac cycle and the flow field at peak diastole during the cardiac cycle (t=0.3 *s*) are shown in figure 2. The velocity profile shows that the velocity deflects towards the inner wall immediately downstream of the bifurcation.

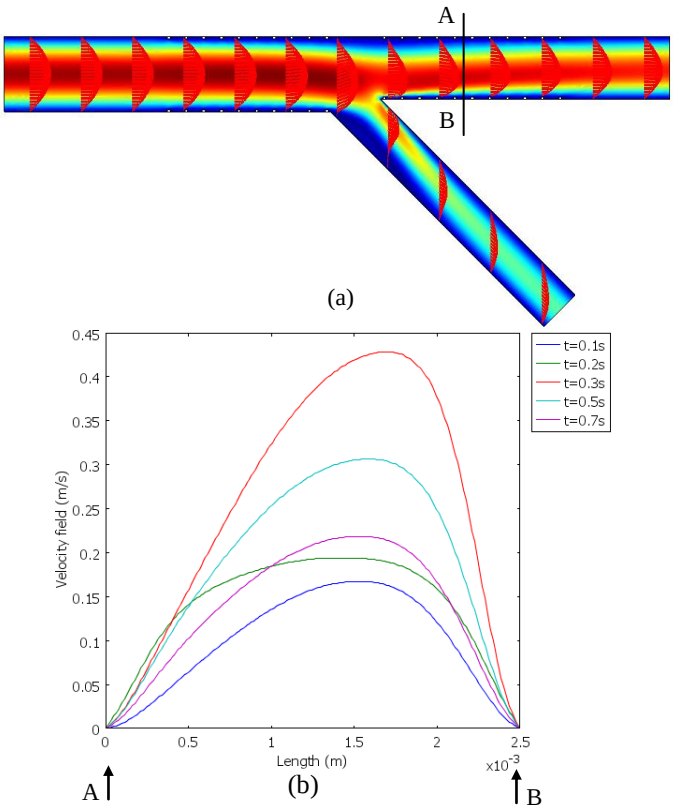

Figure 2. Velocity field in coronary artery bifurcation at peak diastole (a) and velocity profile in section A-B in daughter vessel in a cardiac cycle (b).

Computational flow models have been developed to analyze flow patterns in both un-stented and stented arteries. Distribution of WSS for four consecutive points along the

daughter vessel for non-Newtonian model before stenting is shown in Figure 3.

The magnitude of WSS varies and oscillates with the cardiac cycle because of the pulsatile changes in the velocity and direction of the blood flow.

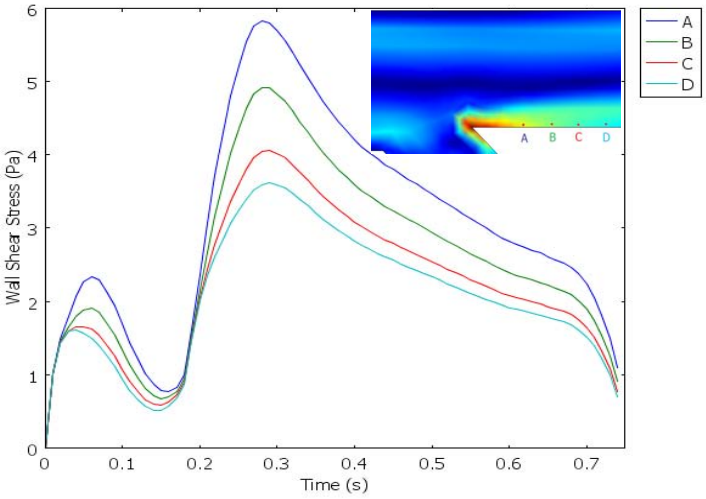

Figure 3. Distribution of WSS for four points on the daughter vessel for non-Newtonian flow before stenting bifurcation in a cardiac cycle.

Following the stent deployment in the arterial wall, the variations of blood velocity can create significant changes in WSS values. Figure 4 shows the variations of WSS for the same four consecutive points on the daughter vessel after stenting bifurcation during one cardiac cycle. The points are in the center of the two adjacent stent and 30 μm downstream of the strut.

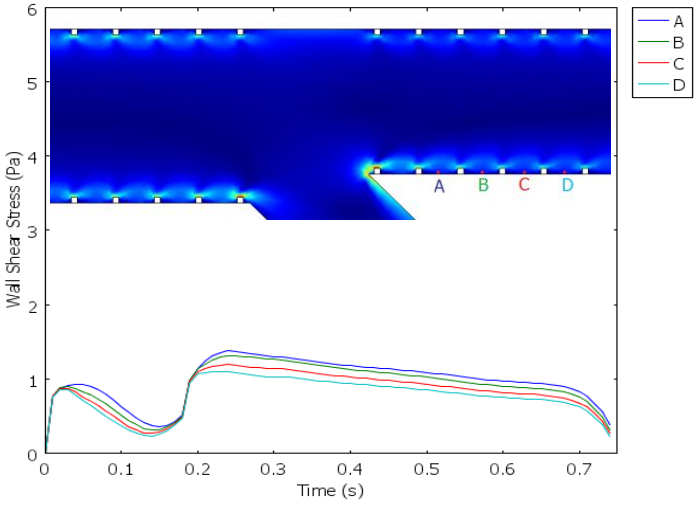

Figure 4. Distribution of WSS for four points on the daughter vessel for non-Newtonian flow after stenting bifurcation in a cardiac cycle.

In the stented region, a significant decrease in the WSS distribution along the arterial wall was observed.

The impact of non-Newtonian flow on the shear stress level between the struts was investigated and the results were obtained for both Newtonian and non-Newtonian models. Figure 5 shows the variations of WSS with respect to time for the four points (A, B, C and D) during a cardiac cycle on the arterial wall. Higher values of WSS are observed for non-Newtonian model as compared to the Newtonian model.

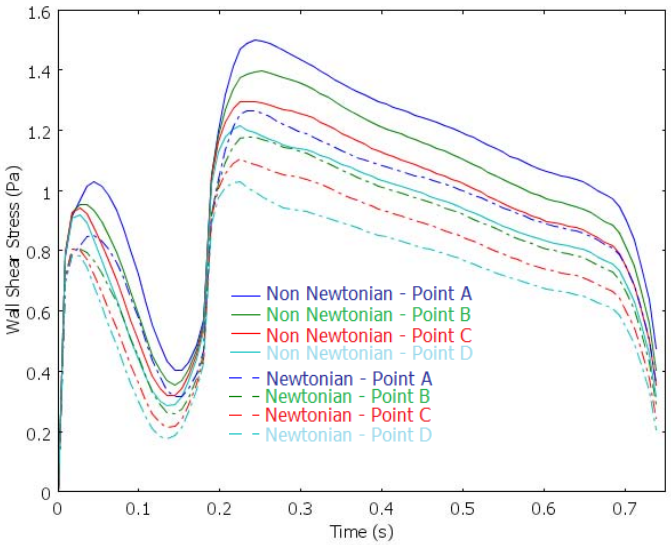

Figure 5. Distributions of WSS for four consecutive points on the daughter vessel for non-Newtonian (solid line) and Newtonian (dashed line) flow condition after stenting bifurcation in a cardiac cycle.

The difference between non-Newtonian and Newtonian models obtained by Benard *et al.* [22] shows the non Newtonian/Newtonian WSS ratio is about 1.5 for single coronary artery. Our numerical results show the non Newtonian/Newtonian WSS ratio of 1.22 for coronary artery bifurcation. The result shows the significant effect of non-Newtonian blood properties on WSS values compared to WSS values obtained from Newtonian analysis regardless of the stent geometry.

Wall shear stress between the stent struts was quantified for five different points which were located at entrance of the intra-stent region, between two stent struts and the point of leaving the intra-stent region. Shear stress distribution for those points between two adjacent stent struts during a cardiac cycle is plotted in Figure (6). High shear stress values are found on or near the stent struts (points A and E).

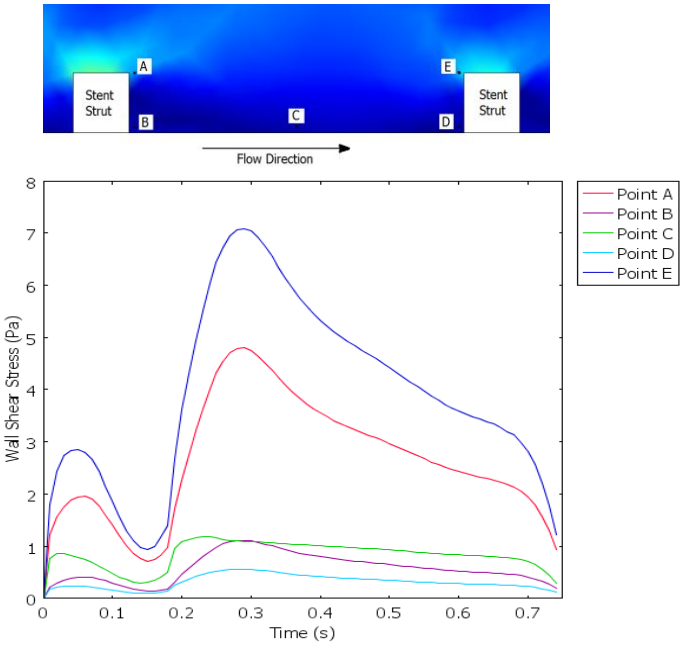

Figure 6. Intra-stent shear stress distribution in a cardiac cycle.

In the stented region and near the arterial wall, there is a significant decrease in the WSS distribution (Points B, C and D). The higher WSS values between two adjacent stent struts correspond to the center part of the region (Point C).

CONCLUSION

This study showed that the rheological properties of blood can significantly affect the flow phenomena in stented bifurcation. Our numerical results for the stented bifurcation showed the non-Newtonian/Newtonian WSS ratio of 1.22 at peak diastole in a cardiac cycle. It indicates that considering the Newtonian property of blood to characterize the flow patterns in the stented arterial segment results in an underestimation of the WSS values.

The results of blood flow dynamic in the stented regions of bifurcation propose that the non-Newtonian property of blood should be taken in to the account for the future stent designs.

RFERENCES

[1] Public Health Agency of Canada, http://www.phac-aspc.gc.ca/ccdpc-cpcmc/topics/cvd-heart-stroke- ng.php

[2] Asakura T., and Karino T., 1990. "Flow patterns and spatial distribution of atherosclerotic lesions in human coronary arteries," *Circulation research*, **66**, pp. 1045-66.

[3] Caro C. G., Fitz-Gerald J. M., and Schroter R. C., 1969. "Arterial wall shear and distribution of early atheroma in man," *Nature*, **223**, pp. 1159-61.

[4] Malek A. M., Alper S. L., and Izumo S., 1999. "Hemodynamic shear stress and its role in atherosclerosis," *Journal of American medical association*, **282**, pp. 2035– 42.

[5] Stone P. H., Coskun A. U., Yeghiazarians Y., *et al.*, 2003. "Prediction of sites of coronary atherosclerosis progression: in vivo profiling of endothelial shear stress, lumen, and outer vessel wall characteristics to predict vascular behavior," *Current opinion in cardiology*, **8**, pp. 458 –70.

[6] Gimbrone M. A. J., Topper J. N., Nagel T., Anderson K. R., and Garcia G., 2000. "Endothelial dysfunction, hemodynamic forces, and atherogenesis," *Annals of the New York academy of sciences*, **902**, pp. 230 –239.

[7] Cunningham K. S., and Gotlieb A. I., 2005. "The role of shear stress in the pathogenesis of atherosclerosis," *Laboratory investigation*, **85**, pp. 9 –23.

[8] Ku D. N., Giddens D. P., Zarins C. K., and Glagov S., 1985. "Pulsatile flow and atherosclerosis in the human carotid bifurcation. Positive correlation between plaque location and low oscillating shear stress," *Arteriosclerosis*, **5**, pp. 293–302.

[9] Moore J. E. J., Xu C., Glagov S., Zarins C. K., and Ku D. N., 1994. "Fluid wall shear stress measurements in a model of the human abdominal aorta: oscillatory ehavior and relationship to atherosclerosis," *Atherosclerosis*, **110**, pp. 225– 40.

[10] Peacock J., Hankins S., Jones T., and Lutz R., 1995. "Flow instabilities induced by coronary artery stents: assessment with an in vitro pulse duplicator," *Biomechanics*, **28**(1), pp. 17– 26.

[11] Nicoud F., Vernhet H., and Dauzat M., 2005. "A numerical assessment of wall shear stress changes after endovascular stenting," *Biomechanics*, **38**, pp. 2019-27.

[12] Fabregues S., Baijens K., Rieu R., and Bergeron P., 1998. "Hemodynamics of endovascular prostheses," *Biomechanics*, **31**(1), pp. 45–54.

[13] Benard N., Coisne D., Donal E., and Perrault R., 2003. "Experimental study of laminar blood flow through an artery treated by a stent implantation: characterization of intra-stent wall shear stress," *Biomechanics*, **36**(7), pp. 991–98.

[14] Ladisa J. F., Guler Jr. I., Olson L. E., Hettrick D. A., Kersten J. R., Warltier D. C., and Pagel P. S., 2003. "Three-dimensional computational fluid dynamics modeling of alterations in coronary wall shear stress produced by Stent Implantation," *Annals of biomedical engineering*, **31**, pp. 972–980.

[15] Kolachalama V. B., Tzafriri A. R., Arifin D. Y., and Edelman E. R., 2009. "Luminal flow patterns dictate arterial drug deposition in stent-based delivery," *Controlled release*, **133**, pp. 24–30.

[16] Deplano V., Bertolotti C., and Barragan P., 2004. "Three-dimensional numerical simulations of physiological flows in a stented coronary bifurcation," *Medical and biological engineering and computing*, **42**, pp. 650-659.

[17] Kaimkhani Z., Ali M., and Faruqui A. M., 2004 "Coronary artery diameter in a cohort of adult Pakistani population," *J Pak Med Assoc.*, **54**(5), pp. 258-61.

[18] Mongrain R., Faik I., Leask R. L., Rodes-Cabau J., Larose E., and Bertrand O. F., 2007. "Effects of diffusion coefficients and struts apposition using numerical simulations for drug eluting coronary stents," *Biomechanical engineering*, **129**, pp. 733-742.

[19] Manfred P., Max O. W., and Sabine W., 1996. "In vitro testing of artificial heart valves: Comparison between Newtonian and non-Newtonian fluids," *International society for artificial organs*, **20**(1), pp. 37-46.

[20] Valencia A., and Baeza F., 2009. "Numerical simulation of fluid–structure interaction in stenotic arteries considering two layer nonlinear anisotropic structural models," *International communications in heat and mass transfer*, **36**(2), pp. 137-142.

[21] Johnston, B. M., Johnston P. R., Corney S., and Kilpatrick D., 2004. "Non-Newtonian blood flow in human right coronary arteries: Transient simulations," *Biomechanics*, **39**(6), pp**.** 1116-1128.

[22] Benard N., Perault R., and Coisne D., 2006. "Computational approach to estimating the effects of blood properties on changes in intra-stent flow," *Annals of biomedical engineering*, **34**(8), pp. 1259–1271.

[23] Faik I., Mongrain R., Leask R. L., Rodes-Cabau J., Larose E., and Bertrand O. F., 2007. "Time-dependent 3D simulations of the hemodynamics in a stented coronary artery," *Biomedical materials*, **2,** pp. 28–37.